

# Ultrafast active plasmonics

Kevin F. MacDonald<sup>1</sup>\*, Zsolt L. Sámson<sup>1</sup>, Mark I. Stockman<sup>2</sup> and Nikolay I. Zheludev<sup>1</sup>

Surface plasmon polaritons, propagating bound oscillations of electrons and light at a metal surface, have great potential as information carriers for next-generation, highly integrated nanophotonic devices<sup>1,2</sup>. Since the term 'active plasmonics' was coined in 2004<sup>3</sup>, a number of techniques for controlling the propagation of guided surface plasmon polariton signals have been demonstrated<sup>4–7</sup>. However, with sub-microsecond or nanosecond response times at best, these techniques are likely to be too slow for future applications in such fields as data transport and processing. Here we report that femtosecond optical frequency plasmon pulses can propagate along a metal–dielectric waveguide and that they can be modulated on the femtosecond timescale by direct ultrafast optical excitation of the metal, thereby offering unprecedented terahertz modulation bandwidth—a speed at least five orders of magnitude faster than existing technologies.

The term 'active plasmonics' was introduced in 2004 in a paper reporting the concept of using optically activated phase-change waveguide materials to control propagating surface plasmon polaritons (SPPs)<sup>3</sup>. Subsequently, reversible changes in waveguide media caused by heating<sup>4,5</sup>, optical excitation of photochromic molecules<sup>6</sup> and interactions mediated by quantum dots<sup>7</sup> have been applied to achieve active modulation of optical-frequency plasmonic signals. However, with switching times no shorter than a few tens of nanoseconds, these are unlikely to satisfy the demands of future chip-scale data transport and integrated nanophotonic applications. Although ultrafast dynamics have been observed for certain plasmon-dependent phenomena, including the extraordinary transmission of sub-wavelength apertures<sup>8,9</sup>, the optical absorption of colloidal metal nanoparticles<sup>10</sup> and optically induced shifting of the Wood's anomalies of gold gratings<sup>11</sup>, the femtosecond optical switching of a propagating SPP signal, as reported here, has not previously been demonstrated.

In essence, we have discovered a nonlinear interaction between a propagating SPP and light that takes place in the skin layer of the metal surface along which the plasmon wave is propagating. A femtosecond optical pulse incident on the metal surface disturbs the equilibrium in the energy–momentum distribution of electrons, thereby influencing SPP propagation along the surface.

We have demonstrated the nonlinear interaction between propagating SPP waves and light in a pump–probe experiment in which a pulsed plasmonic probe signal was generated on an aluminium/silica interface by grating coupling from a pulsed 780-nm laser beam. After travelling 5  $\mu\text{m}$  across the unstructured interface (a distance comparable to the SPP decay length), the plasmon wave was decoupled to light by another grating and subsequently detected. Optical control (pump) pulses, originating from the same laser, were incident on the waveguide region between the coupling and decoupling gratings (see Fig. 1). The transient effect of control pulse excitation on the propagation of the SPP signal was monitored by varying the time delay between the SPP excitation and optical pump pulses. It was found that an optical pump fluence of about

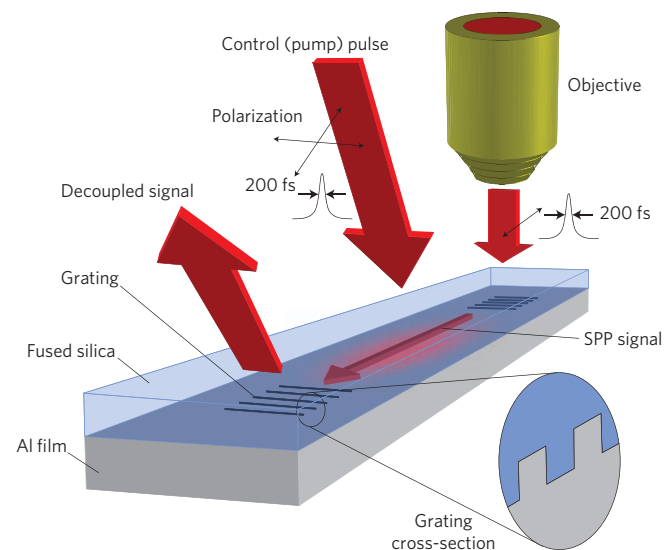


**Figure 1 | Ultrafast optical modulation of SPP propagation.** A plasmonic signal, coupled to and from the waveguide by gratings on an aluminium/silica interface, is modulated by optical pump pulses as it travels between the gratings.

10  $\text{mJ cm}^{-2}$  leads to around 7.5% modulation of the plasmon wave intensity.

The experiments used nearly transform-limited 200 fs optical pulses with a spectrum centred at 780 nm. The photon energy of the optical radiation ( $\hbar\omega = 1.59$  eV) was therefore close to the interband absorption peak in aluminium ( $\hbar\omega \sim 1.55$  eV), the metal component of the plasmon waveguide. Group velocity dispersion for the plasmonic signal is close to zero in this spectral range, and pulse broadening during propagation between the gratings is estimated to be no more than a few femtoseconds. With an electron configuration of  $[\text{Ne}]3s^23p^1$ , aluminium is a classic example of a free-electron metal in which the absorption spectrum is modified by interband transitions. Its optical interband absorption originates mainly from transitions between parallel bands  $\Sigma_3 - \Sigma_1$  in the vicinity of the  $\Sigma$  [110] axis, near the  $K$  point (see Fig. 2a and ref. 12).

Two experimental configurations were used. In the first, the linear polarization direction of the pump field was in the plane of incidence containing the SPP propagation direction and was thus predominantly in the direction of the electron oscillations in the SPP wave (Fig. 2b). In the second configuration, the pump field polarization was perpendicular to the plane of incidence and was thus perpendicular to the electron oscillations in the plasmon wave (Fig. 2c).

The experimental results are summarized in Fig. 3, which shows the effect that the pump pulses have on the amplitude of the decoupled plasmonic signal as a function of pump–probe delay

<sup>1</sup>Optoelectronics Research Centre, University of Southampton, Highfield, Southampton, Hampshire, SO17 1BJ, UK, <sup>2</sup>Department of Physics and Astronomy, Georgia State University, 29 Peachtree Center Avenue, Atlanta, Georgia 30303-4106, USA; \*e-mail: kfm@orc.soton.ac.uk

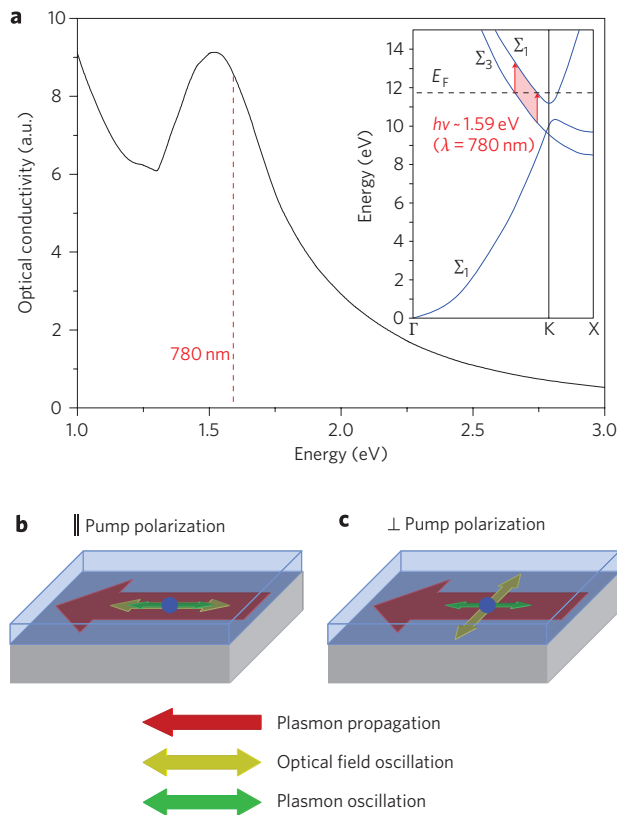


**Figure 2 | SPP modulation through optical excitation of aluminium.**

**a**, Dispersion of the optical conductivity of aluminium showing the interband absorption peak. The inset shows the relevant part of the metal's band structure. **b,c**, The two experimentally investigated configurations of pump pulse polarization and plasmonic electron oscillation directions.

time (Figs. 3a, b) and pump fluence (Fig. 3c). 'Fast' and 'slow' components of the transient pump-probe interaction have been observed. In all cases the presence of the pump pulse increases the magnitude of the transmitted plasmonic signal. The fast component replicates the optical cross-correlation function of the pump and probe pulses (Fig. 3a), but is only seen in the first experimental configuration where the pump polarization has a component parallel to the direction of SPP propagation. The magnitude of this fast SPP signal modulation component reaches a level of around 7.5% for pump pulse fluences of  $10 \text{ mJ cm}^{-2}$  (Fig. 3c). The slow component of the transient response is present in both experimental configurations, that is, for pump polarization directions both parallel and perpendicular to the SPP propagation direction. It grows for around 2 ps during and after a pump pulse then begins to relax with a characteristic decay time of about 60 ps (Fig. 3b). The magnitude of this slow SPP modulation reaches about 4% at a pump fluence of  $10 \text{ mJ cm}^{-2}$  (Fig. 3c).

In summary, the transient response data indicate that there are two components to the nonlinear response: a fast component with a relaxation time shorter than the 200-fs pulse duration and a slow component with a relaxation time of about 60 ps. The fast component is sensitive to the mutual orientation of the pump beam's polarization state and the electron oscillation direction in the signal plasmon wave.

We believe that on the microscopic level the mechanisms underpinning the reported plasmon modulation effect are related to those responsible for transient changes in the optical properties of metal nanoparticles<sup>10</sup>, in the Wood's anomalies of gold gratings<sup>11</sup>, and in particular in the reflectivity of aluminium<sup>13,14</sup>, as observed in femtosecond pump-probe experiments. Indeed, any pump-induced variation in refractive index  $N = n + ik$  will simultaneously

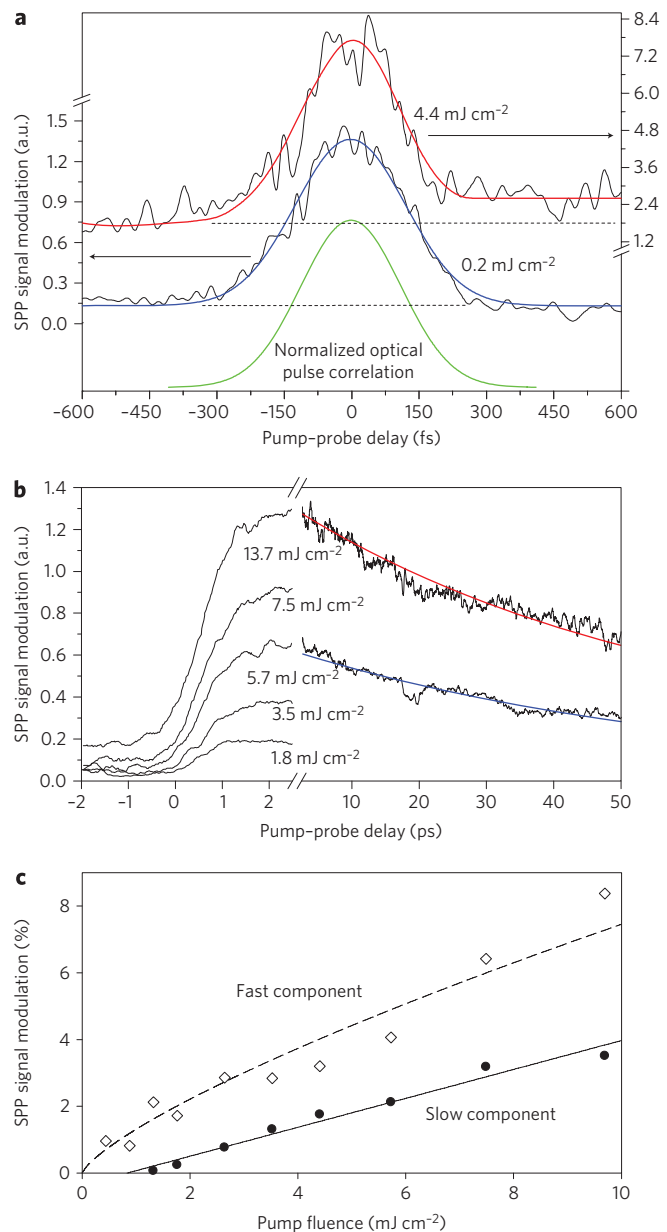


**Figure 3 | Ultrafast SPP modulation dynamics and pump fluence scaling.**

**a,b**, Transient pump-induced changes in the decoupled plasmonic signal for pump light polarized parallel (**a**, alongside a normalized trace, in green, of the optical pulse correlation), and perpendicular (**b**, for a range of pump fluences as labelled) to the SPP propagation direction. **c**, Corresponding peak magnitudes of the fast and slow pump-induced modulation components as a function of pump pulse fluence.

lead to a change in reflectivity  $R$  and plasmon decay length  $L$ . For metals it is generally true that  $k > n$  and aluminium is no exception at the experimental wavelength  $\lambda = 780 \text{ nm}$ . Under such conditions,  $(\partial L/\partial n)$  and  $(\partial R/\partial n)$  have the same sign, as do  $(\partial L/\partial k)$  and  $(\partial R/\partial k)$ .

The connection between light-induced reflectivity increases and plasmonic signal propagation may also be illustrated using the Drude model, within which it is found that a 7% change in the density of free carriers (induced by pump pulse excitation) gives an increase of 7.5% in the detected plasmon signal intensity (as observed at a fluence of  $10 \text{ mJ cm}^{-2}$ ) by increasing the plasmon decay length. This increase in free carrier density simultaneously produces an increase of 0.48% in the reflectivity of the

aluminium/silica interface. These figures are consistent with prior studies that, for example, have demonstrated a reflectivity increase of  $\sim 0.8\%$  at a fluence of  $10 \text{ mJ cm}^{-2}$  (ref. 13), and an increase of  $\sim 0.1\%$  at about  $1 \text{ mJ cm}^{-2}$  (ref. 14).

A fast, polarization-sensitive increase in aluminium reflectivity has previously been observed in optical pump–probe experiments<sup>14</sup>, and as for the present case of light–SPP interaction it appeared only for parallel pump and probe polarizations. This zero-delay spike, which is also routinely seen in other metals, is due to a combination of a coherent nonlinearity and coupling of the wavelength degenerate pump into the probe through a transient grating created by the pump beam and probe SPP wave. The coherent nonlinearity is linked to anharmonic components of plasmonic oscillation resulting from the non-parabolicity of the electron dispersion. As argued in ref. 15, with increasing excitation, additional nonlinear mechanisms are activated and damping of the SPP increases, giving rise to the observed sublinear increase in the magnitude of the fast component with pump fluence (Fig. 3c). The disappearance of the fast component for perpendicular polarizations is characteristic of a nonlinearity related to the non-parabolicity of free electron dispersion. It occurs for the same reasons that the third harmonic generated on reflection from a free-electron metal surface has the same polarization as the pump<sup>16</sup>.

The slow component of the interaction between optical pump and SPP probe pulses shows no discernable dependence on the mutual orientation of pump and probe polarizations. It has the same origin as the slow transient reflectivity change observed in aluminium<sup>13</sup>, in that when an intense pump pulse excites numerous electrons to states above the Fermi level through an interband transition, a transient response known as the ‘Fermi smearing’ nonlinearity<sup>17</sup> occurs rapidly then disappears as electrons thermalize with the lattice. Subsequent changes in the dielectric coefficients are essentially of a thermal and elastic nature. In this case the relaxation time of the response is related to the time needed for heat to leave the metal’s skin layer and for the lattice deformation to recover. We argue that the increasing magnitude of the slow response component observed during the first two picoseconds after excitation (see Fig. 3b) is related to a dynamic balance between Fermi smearing and thermal/elastic effects, while the observed relaxation time of  $\sim 60 \text{ ps}$  is related to the thermal and elastic transients in the skin layer and is in full agreement with ref. 18.

Advantages of the present switching technology for plasmon-polariton signals include simplicity of both geometry and material composition (including a notable lack of organic components susceptible to photo-degradation), compatibility with existing CMOS fabrication techniques, and an operational wavelength close to an important on-chip interconnect wavelength. It should be noted that the level of direct plasmonic signal modulation may be increased manyfold using interferometric arrangements, as demonstrated in plasmonic versions of Mach–Zehnder<sup>4</sup> and Fabry–Perot<sup>7</sup> interferometers. The demonstrated switching time is around  $200 \text{ fs}$ , but could be as short as a few tens of femtoseconds as it is ultimately limited only by the electron momentum relaxation time. This is radically faster than the millisecond response time of thermo-plasmonic modulators<sup>4,5</sup>. The required excitation level compares favorably with the optical fluence of  $\sim 15 \text{ mJ cm}^{-2}$  required to control a plasmonic gate based on structural phase switching in a gallium plasmon waveguide, where switching times of about  $50 \text{ ns}$  are achieved<sup>19</sup>. The switching fluence for an optical pulse acting directly on the aluminium waveguide is a factor of a hundred higher than required in a plasmonic modulator exploiting CdSe quantum dots to control SPP losses, but the  $200\text{-fs}$  switching time achieved in the present study is more than five orders of magnitude shorter than the  $40\text{-ns}$  switching time reported for the quantum dot device<sup>7</sup>. In the opposite corner of the energy versus speed parameter map, the power requirements for photochromic molecular

switching of plasmons<sup>6</sup> are in the milliwatt range, but with cycle times of tens of seconds this technology is probably better suited to data storage applications. Among other potential candidates for active plasmonics are J-aggregates with picosecond response and relaxation times<sup>9</sup>, but their application to the control of guided plasmonic modes is yet to be demonstrated.

The ultrafast femtosecond switching times and modest switching energy requirements (comparable with those needed to record information bits on a CD) reported here open the gates to the exploration of what can ultimately be achieved in nonlinear plasmonics<sup>20</sup> and active plasmonic switching, in particular for the purposes of high-bandwidth interconnects, plasmon-polariton modulation, all-plasmonic switching<sup>21</sup>, and pulse shaping and self-modulation through the use of nonlinear propagation regimes. In particular, the availability of the ultrafast nonlinearity discovered in this work may act as a starting point for the exciting challenge of exploring information transfer using plasmon-polariton analogues of optical solitons, that is, plasmon-solitons, exploiting the nonlinearity of the metal rather than the dielectric waveguide component<sup>22</sup>. We believe that such studies will inform the future development of technologically relevant device structures and operational modes for plasmonics in the same way that studies of ultrafast and nonlinear optical phenomena have contributed to the advancement of photonics, most notably in the form of today’s fibre-based telecommunications networks.

In summary, we report the first experimental evidence that femtosecond plasmon pulses can be generated, transmitted, modulated and decoupled for detection in a single device, and describe a new principle for the direct optical modulation of plasmon signals with terahertz bandwidth that is supported by experimental demonstration.

## Methods

The waveguide structure and grating patterns were fabricated on optically polished fused silica substrates using electron-beam lithography and anisotropic reactive ion etching. Grating structures were etched into the silica to a nominal depth of  $43 \text{ nm}$  with areas between the gratings masked. The fabrication was completed with the evaporation of a  $250\text{-nm}$  aluminium layer to form an optically flat metal/silica plasmon waveguide interface.

The plasmonic probe signal was generated on the aluminium/silica interface by grating coupling from a normally incident  $780\text{-nm}$  pulsed laser beam and detected in the optical far field after decoupling at an oblique angle by a second grating separated from the first by  $5 \mu\text{m}$  of unstructured metal/dielectric interface (a distance comparable to the SPP decay length). The coupling and decoupling gratings, each comprising 40 lines, had periods of  $0.522 \mu\text{m}$  (optimized for normal incidence coupling) and  $1.184 \mu\text{m}$  (giving an output beam angle of  $54^\circ$  after refraction at the silica/air interface), respectively. The beam from an amplified mode-locked Ti:sapphire laser (Coherent Mira + RegA) tuned to a centre wavelength of  $780 \text{ nm}$ , generating pulses with a duration of  $200 \text{ fs}$  at a rate of  $250 \text{ kHz}$ , was split into pump and probe components, which were modulated at different frequencies ( $\nu_1$  and  $\nu_2$ ). The probe beam, polarized parallel to the grating vectors as required for coupling to a plasmon wave, was directed at normal incidence via a  $10\times$  long working distance objective, to a  $17\text{-}\mu\text{m}$ -diameter spot with a fluence of  $0.9 \text{ mJ cm}^{-2}$  onto the coupling grating. The decoupled signal was monitored using a silicon photodetector and lock-in amplifier. The linearly polarized pump beam was focused onto the sample at an oblique angle ( $27^\circ$ ) to a spot with a diameter of  $34 \mu\text{m}$  centred on the unstructured region between the coupling and decoupling gratings. An optical delay line was used to vary the arrival time of pump pulses at the sample relative to the corresponding probe pulses, and the transient effect of pump excitation on the propagation of the probe SPP signal was monitored by recording the magnitude of the decoupled optical signal at the chopping sum frequency ( $\nu_1 + \nu_2$ ) as a function of pump–probe delay.

Variations in reflectivity  $R = ((1 - n)^2 + k^2)/((1 + n)^2 + k^2)$  and plasmon decay length  $L = (\lambda/2\pi) \times (n^2 - k^2)^2/2nk$  with refractive index  $N + n + ik$  are given by the following formulae:

$$\delta R = \frac{4}{(n^2 + k^2 + 2n + 1)^2} \times [(n^2 - k^2 - 1)\delta n + (2nk)\delta k]$$

$$\delta L = \frac{\lambda(n^2 - k^2)}{4\pi n^2 k^2} \times [(3n^2 k + k^3)\delta n - (3nk^2 + n^3)\delta k]$$

Received 16 July 2008; accepted 10 November 2008;  
published online 14 December 2008

## References

1. Atwater, H. A. The promise of plasmonics. *Sci. Am.* **296**, 56–63 (April 2007).
2. Ozbay, E. Plasmonics: Merging photonics and electronics at nanoscale dimensions. *Science* **311**, 189–193 (2006).
3. Krasavin, A. V. & Zheludev, N. I. Active plasmonics: Controlling signals in Au/Ga waveguide using nanoscale structural transformations. *Appl. Phys. Lett.* **84**, 1416–1418 (2004).
4. Nikolajsen, T., Leosson, K. & Bozhevolnyi, S. I. Surface plasmon polariton based modulators and switches operating at telecom wavelengths. *Appl. Phys. Lett.* **85**, 5833–5835 (2004).
5. Lereu, A. L., Passian, A., Goudonnet, J.-P., Thundat, T. & Ferrell, T. L. Optical modulation processes in thin films based on thermal effects of surface plasmons. *Appl. Phys. Lett.* **86**, 154101 (2005).
6. Pala, R. A., Shimizu, K. T., Melosh, N. A. & Brongersma, M. L. A nonvolatile plasmonic switch employing photochromic molecules. *Nano Lett.* **8**, 1506–1510 (2008).
7. Pacifici, D., Lezec, H. J. & Atwater, H. A. All-optical modulation by plasmonic excitation of CdSe quantum dots. *Nature Photon.* **1**, 402–406 (2007).
8. Hendry, E. *et al.* Optical control over surface-plasmon-polariton-assisted THz transmission through a slit aperture. *Phys. Rev. Lett.* **100**, 123901 (2008).
9. Dintinger, J., Robel, I., Kamat, P. V., Genet, C. & Ebbesen, T. W. Terahertz all-optical molecule-plasmon modulation. *Adv. Mater.* **18**, 1645–1648 (2006).
10. Link, S. & El-Sayed, M. A. Spectral properties and relaxation dynamics of surface plasmon electronic oscillations in gold and silver nanodots and nanorods. *J. Phys. Chem. B* **103**, 8410–8426 (1999).
11. Rotenberg, N., Betz, M. & van Driel, H. M. Ultrafast control of grating-assisted light coupling to surface plasmons. *Opt. Lett.* **33**, 2137–2139 (2008).
12. Segall, B. Energy bands of aluminum. *Phys. Rev.* **124**, 1797–1806 (1961).
13. Guo, C., Rodriguez, G., Lobad, A. & Taylor, A. J. Structural phase transition of aluminum induced by electronic excitation. *Phys. Rev. Lett.* **84**, 4493–4496 (2000).
14. Wilks, R. & Hicken, R. J. Transient optical polarization response of aluminium at an interband transition. *J. Phys.: Condens. Matter.* **16**, 4607–4617 (2004).
15. Park, S., Pelton, M., Liu, M., Guyot-Sionnest, P. & Scherer, N. F. Ultrafast resonant dynamics of surface plasmons in gold nanorods. *J. Phys. Chem. C* **111**, 116–123 (2007).
16. Georges, A. T. Coherent and incoherent multiple-harmonic generation from metal surfaces. *Phys. Rev. A* **54**, 2412–2418 (1996).
17. Eesley, G. L. Generation of nonequilibrium electron and lattice temperatures in copper by picosecond laser pulses. *Phys. Rev. B* **33**, 2144–2151 (1986).
18. Richardson, C. J. K. & Spicer, J. B. Short-time thermoelastic contributions to picosecond-time scale reflectivity measurements of metals. *Appl. Phys. Lett.* **80**, 2895–2898 (2002).
19. Krasavin, A. V., MacDonald, K. F., Zheludev, N. I. & Zayats, A. V. High-contrast modulation of light with light by control of surface plasmon polariton wave coupling. *Appl. Phys. Lett.* **85**, 3369–3371 (2004).
20. Palomba, S. & Novotny, L. Nonlinear excitation of surface plasmon polaritons by four-wave mixing. *Phys. Rev. Lett.* **101**, 056802 (2008).
21. Krasavin, A. V., Zayats, A. V. & Zheludev, N. I. Active control of surface plasmon-polariton waves. *J. Opt. A: Pure Appl. Opt.* **7**, S85–S89 (2005).
22. Feigenbaum, E. & Orenstein, M. Plasmon-soliton. *Opt. Lett.* **32**, 674–676 (2007).

## Acknowledgements

This work was supported by the Engineering and Physical Sciences Research Council (UK), the Department of Energy and National Science Foundation (USA), and the United States–Israel Binational Science Foundation. The authors would like to acknowledge the technical assistance of J.D. Mills.

## Additional information

Reprints and permission information is available online at <http://npg.nature.com/reprintsandpermissions/>. Correspondence and requests for materials should be addressed to K.F.M.